IEEE Open Journal of
Power Electronics

Received 16 June 2020; revised 23 July 2020; accepted 30 July 2020. Date of publication 5 August 2020;
date of current version 17 August 2020. The review of this article was arranged by Associate Editor Xiong Du.

Digital Object Identifier 10.1109/OJPEL.2020.3014443

Junction Temperature Control System to Increase the Lifetime of IGBT-Power-Modules in Synchronous Motor Drives Without Affecting Torque and Speed

JULIAN WÖLFLE, MAXIMILIAN NITZSCHE (Student Member, IEEE), JOHANNES RUTHARDT, AND JÖRG ROTH-STIELOW (Member, IEEE)

Institute for Power Electronics and Electrical Drives, University of Stuttgart, 70569 Stuttgart, Germany

CORRESPONDING AUTHOR: MAXIMILIAN NITZSCHE (e-mail: nitzsche@ilea.uni-stuttgart.de)

ABSTRACT Load changes of electrical machines driven by inverters cause temperature swings of the semiconductor devices in IGBT modules of the inverters. These temperature swings lead to mechanical strain in the different material layers of the IGBT-power-modules and limit the numbers of cycles to failure and therefore reduce the lifetime of the IGBTs. This paper presents a temperature control system which is paralleled to the standard torque control system. It aims to reduce the magnitude of temperature swings of the semiconductor devices of IGBT modules caused by load changes of an interior permanent magnet synchronous machine. The principle method is, to increase the temperature of the semiconductor devices of the IGBT-modules by creating higher power losses during low load conditions of the machine without affecting torque and speed. This reduces the magnitude of the load induced temperature swings of the semiconductor devices of IGBT-modules and increases its lifetime at the cost of increased power losses. Three variables have been identified that influence the power losses in inverter modules without necessarily affecting the output power of the permanent synchronous machine. These variables are switching frequency of the inverter, length of the clamping area when a discontinuous modulation is applied and the reactive component of the inverter current. The influence of each variable which regards to the losses in the IGBT-power-modules is explained and the related control methodology is described. The analytic results are verified by experimental results obtained from a test set up.

INDEX TERMS Artificially increased losses, discontinuous modulation, extra loss creation, IGBT lifetime, junction temperature control, paralleled temperature control system, reactive current, reduction of temperature swing, variable switching frequency.

I. INTRODUCTION

The main requirements for power electronic devices and systems are functionality, efficiency and lifetime. This paper focuses on the increase of the lifetime of the semiconductor devices in IGBT-power-modules. Environmental impact factors affecting lifetime are cosmic radiation, humidity, mechanical vibration, and temperature. For these impact factors accelerated lifetime tests are well established [1]. In many applications the important impact factor on lifetime of IGBT-power-modules is the operating junction temperature of the semiconductor devices. The temperature swing $\Delta\vartheta_\mathrm{j}$ itself, as well as the mean value $\vartheta_\mathrm{j,m}$ of the semiconductor's junction temperature have an influence on the number of cycles to failure N_f and therefore on the lifetime of the semiconductor device. This is well established and documented in the LESIT study [2], see Fig. 1.

The reasons for this are the various layers of materials in the IGBT-module with different coefficients of thermal expansion (CTE) which leads to mechanical strains. This leads to material fatigue [3] and a decay in the lifetime of the device.

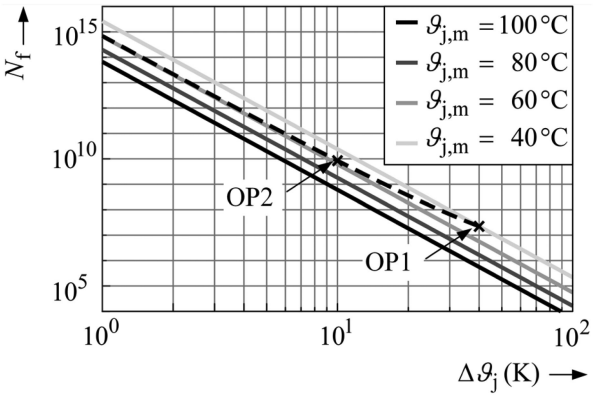

FIGURE 1. Cycles to failure N_f of IGBT-power-modules as a function of $\Delta\vartheta_j$ and $\vartheta_{j,m}$ provided by LESIT study [2].

The LESIT lifetime model [2] considers the temperature swing $\Delta\vartheta_j$ and the mean junction temperature $\vartheta_{j,m}$ of the device under test as major parameters. Experimental results of LESIT are approximated by Eqn. 1, where N_f is the number of switching cycles until failure, which is more or less equivalent to life expectancy.

$$N_f = A \cdot \Delta\vartheta_j^{\alpha} \cdot e^{\left(\frac{E_a}{k_B \cdot \vartheta_{j,m}}\right)} \tag{1}$$

The parameters of the activation energy E_a, A and α are defined in [1] for the LESIT lifetime model, k_B is the "Boltzmann"-constant. Fig. 1 illustrates that a reduced temperature swing leads to higher lifetime expectancy of the IGBT-power-modules.

A common approach is to increase lifetime by reducing temperatures by minimizing losses and optimizing heat dissipation [4]–[8]. In many applications this can't be achieved. Other approaches however, do not reduce the junction temperature swings $\Delta\vartheta_j$ by reducing the power losses during high load conditions but by increasing the power losses [9], [10] during low load conditions.

In this paper a temperature control system is described which decreases the temperature swings of the semiconductor devices in IGBT-power-modules by increasing power dissipation during low load conditions in a three-phase inverter without materially affecting the mechanical output parameters of the interior permanent magnet synchronous machine supplied by the three-phase inverter. This is achieved by paralleling this temperature control system to the torque control system.

The solid lines in Fig. 1 show the number of thermal cycles to failure at a constant mean temperature. The dashed line shows the number of cycles for a constant maximum temperature within the cycles. With the proposed control strategy, the operation points are shifted along this dashed line towards higher numbers of cycles to failure as the following example explains.

While additional power dissipation during low load conditions inevitably increases the mean temperature $\vartheta_{j,m}$ which decreases the number of cycles to failure N_f. But the impact of the reduction in temperature swing $\Delta\vartheta_j$ is predominant and leads to an overall increased number of cycles to failure N_f and therefore the expected lifetime is increased in accordance to the LESIT study findings. This is illustrated in Fig. 1 with the two operation points OP1 and OP2. The operation point OP1 represents an example for an IGBT-power-module in a specific application with a maximum junction temperature of 60 °C at maximum load and a minimum junction temperature of 20 °C at minimum load, leading to a junction temperature swing $\Delta\vartheta_j$ of 40 K and an average junction temperature $\vartheta_{j,m}$ of 40 °C. If the minimum junction temperature in this example is increased by additional power dissipation within the power module during minimum load condition, the minimum junction temperature could be lifted from 20 °C to 50 °C and hence the temperature swing would decrease from 30 K to 10 K while the average junction temperature $\vartheta_{j,m}$ would increase from 40 °C to 55 °C. This operation point is shown as OP 2 in Fig. 1. In both cases the maximum temperature is still 60 °C if the thermal time constants of the semiconductor devices setup in the IGBT-module are considerable smaller than the time duration of the load changes. At operation point OP2 the expected number of cycles to failure N_f is about 200 times bigger than in operation point OP1. As a result, the expected life time is considerably increased.

The analysis of this example shows in principle, that it is possible, to increase the lifetime and therefore the reliability of the IGBT-module by increasing the power losses during low load conditions in order to reduce the junction temperature swing [11]–[14].

Besides the control strategy, it is important to find a suitable control variable to influence the junction temperature over a wide range. For this, a variable cooling system is used in [15]. The disadvantage is, that special power modules are required and the hardware effort is large. In other works, gate drivers are presented and investigated, which are able to affect switching and conduction losses to influence the junction temperature [16]–[21]. These approaches are flexible because each power semiconductor devices' junction temperature can be influenced independently. However, it is difficult to implement because special gate drivers are required.

In some applications it is possible to apply a reactive current, which affects the losses and hence the junction temperature in converters [13], [22]. Special modulation techniques are also an option to vary power losses [21], [23]–[26]. These methods are especially suitable for specific applications (e.g., wind energy) or converters.

This paper presents analysis, evaluation and experimental verification of three different control variables and finally a combination of them for increasing the junction temperature of the semiconductor devices within the IGBT-power-modules during low load conditions with the aim of reducing the temperature swings and consequently increasing the lifetime expectancy of the IGBT-power-modules. The three control variables are (a): Increase in the switching frequency f_{pwm}, (b): Discontinuous modulation technique which enables the

possibility to reduce the length of the clamping areas φ_A and (c): Increase the reactive component of the motor current i_{rec}.

The main advantage of the proposed control system for junction temperature control is, that all three methods, when properly applied, do not affect the mechanical output power of the interior permanent synchronous machine. In addition, they are easy to implement and do not require additional hardware compared to many approaches mentioned before.

In order to influence and control the junction temperature of a semiconductor device in an IGBT-power-module, this temperature must be established first. This can be done by direct measurement (interference with the semiconductor device), by indirect measurement (monitor temperature sensible parameters of the semiconductor device), by reading an approximate temperature from an integrated sensor, or the semiconductor temperature can be calculated with device parameters and the operational values of current and voltage. For ease of implementation and avoiding interference with the IGBT-power-module and its required high voltage insulation, the junction temperatures of the semiconductor devices (IGBTs and diodes) of the IGBT-power-modules are instantly calculated within the control system instead. The advantage is the simple implementation with a microprocessor without any other additional hardware. Therefore, it is suitable for implementation in standard applications. The details of the calculations and the thermal models used are explained in detail in [12]–[14], [23].

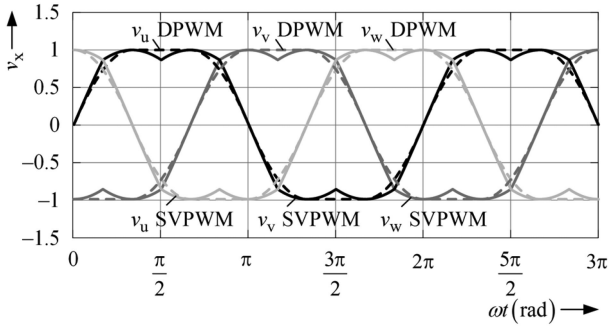

FIGURE 2. Reference voltages for SVPWM and DPWM at $m = \frac{2}{\sqrt{3}}$.

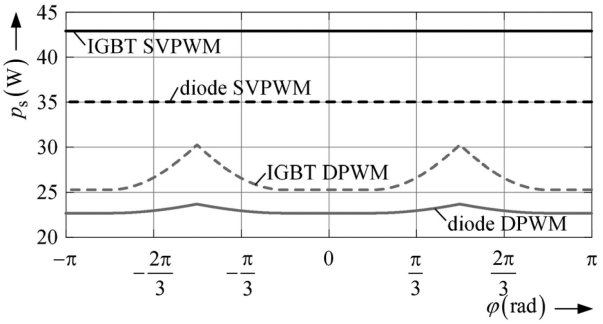

FIGURE 3. Switching losses of SVPWM and DPWM at $\hat{i} = 25\mathrm{A}$ and at $m = \frac{2}{\sqrt{3}}$.

II. CONTROL VARIABLES

The switching frequency of IGBT-power-modules in an inverter is set as high as possible for reasons of low ripple in the three-phase output current, but also set as low as possible on the other side for low switching power losses on the semiconductor devices. In fact, the switching losses can be manipulated by changing the switching frequency f_{PWM}, leading to more or less switching actions within a fundamental period of the output phase current [11], [12].

A second possibility to influence the number of switching actions can also be achieved by changing to different modulation strategies [9] or using a hybrid discontinuous modulation strategy [23]. The hybrid discontinuous modulation strategy was used in this paper and the basic principles will be explained in the following. The space vector pulse width modulation strategy (SVPWM) is a modulation technique where the semiconductor devices switch during the entire fundamental period of the output current. The maximum modulation range is $m = \frac{2}{\sqrt{3}}$. Discontinuous pulse width modulation strategies [27] (DPWM max, min, 0, 1, 2 or 3) on the other hand enable the possibility to reduce the number of switching actions within a period by clamping the voltage by the semiconductor devices to the positive or negative DC-link leading to full conduction. Depending on the DPWM strategy the length of the clamping area is fixed for values of $\frac{\pi}{6}$, $\frac{\pi}{3}$ or $\frac{2\pi}{3}$ within a half of a period. Therefore, there is a reduction of the number of switching actions by a fixed number. The DPWM strategy which sets a clamping length of $\frac{\pi}{3}$ also enables the possibility to shift the position of the clamping area between $-\frac{\pi}{6}$ and $\frac{\pi}{6}$ [28].

This property can be used to minimize the switching losses, if possible, by shifting the clamping area φ_A in dependence of the phase shift φ between the fundamentals of the output currents and voltages. The maximal modulation range is the same as by the SVPWM strategy ($m = \frac{2}{\sqrt{3}}$). The reference voltages $v_x \in (u, v, w)$ of both modulation techniques at maximal modulation range are depicted in Fig. 2.

The mean switching losses p_s and conduction losses p_c as a function of the phase shift φ of both modulation strategies for a fixed current amplitude of $\hat{i} = 25\,\mathrm{A}$, a DC-link voltage of $V_{DC} = 400\mathrm{V}$ and at a switching frequency of $f_{PWM} = 25\,\mathrm{kHz}$ are shown in Figs. 3 and 4.

It is visible that there is very little difference in conduction losses p_c, however the switching losses p_s do show a significant difference. It is worth mentioning that the difference depends on the actual current amplitude $\hat{i}$. A combination of these modulation strategies leads to a hybrid discontinuous pulse width modulation strategy (HDPWM). Due to the combination it is possible to choose a variable length of the clamping area φ_A between 0 and $\frac{\pi}{3}$. If a clamping length smaller than $\frac{\pi}{3}$ is chosen then the remaining areas left and right of the length of the clamping area φ_A must be replaced by the

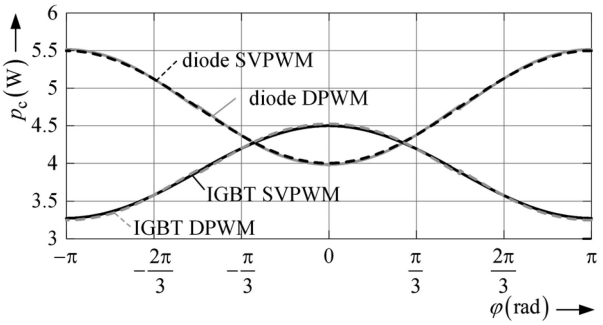

FIGURE 4. Conduction losses of SVPWM and DPWM at $\hat{i} = 25$ A and at $m = \frac{2}{\sqrt{3}}$.

TABLE 1. Parameters IPMSM

Symbol	Quantity	Value
R_S	stator resistance	9.3 mΩ
L_d	direct inductance	80 µH
L_q	quadrature inductance	410 µH
ψ_{PM}	flux linkage	58.1 mVs
z_p	pole pairs	4
t_{rated}	rated torque	134 Nm
P_{rated}	rated power	70 kW
n_{rated}	rated speed	5500 rpm

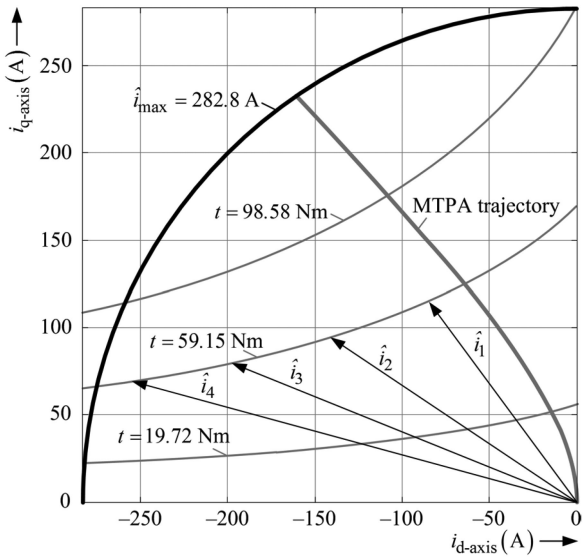

FIGURE 5. MTPA trajectory, torque, current limitation circle for the IPMSM.

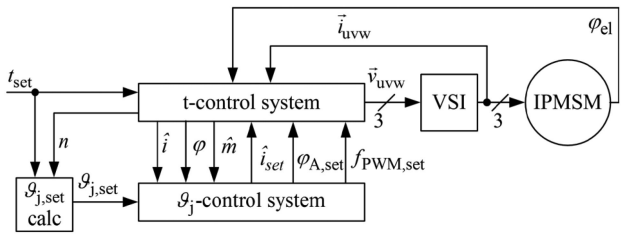

FIGURE 6. Overview of the combined total control system.

SVPWM strategy. With this modulation strategy a second control variable exists to influence the switching losses p_s.

The drawback of using the two previous mentioned control variables (f_{PWM}, φ_A) for control is, that an output current amplitude $\hat{i}$ is required in order to produce any power losses at all. The conduction losses p_c can only be influenced by pre-setting an additional current through the semiconductor devices. This current has to be a reactive current i_{rec}, if the temperature control system is not to have an influence on the demanded output power of the machine supplied. In this work an interior permanent synchronous machine (IPMSM) is used, see Table I. The current controllers operate the IPMSM in field orientated coordinates and Fig. 5 depicts exemplary torque hyperbolics, the current amplitude limitation circle, and the maximum torque per current trajectory (MTPA) in field orientated coordinates.

It is evident that the same torque can be achieved with different current amplitudes $\hat{i}$. This can be used to have a current through the power modules even at zero torque conditions. The junction temperature control system is active only, when the IPMSM is at speed and therefore a three-phase alternating current system exists. The variables to be influenced by the controller have an unwanted influence on the power losses in the IPMSM.

III. TEMPERATURE CONTROL SYSTEM

The temperature control system aims to reduce the swing of the junction temperatures of the semiconductor devices within the IGBT-power-modules by reducing the temperature swing during low load conditions by artificially increasing the losses of the semiconductor devices, while a torque control system maintains the set torque t_{set}. Both control systems work in parallel as shown in Fig. 6.

The torque control system requires the electrical orientation angle φ_{el} of the IPMSM and the phase currents $i_{u,v,w}$ of the three-phase inverter. The actual speed is calculated by an observer fed by the actual electrical orientation angle φ_{el}. The current set value calculation requires the desired torque t_{set} and the actual speed n. The torque control system operates in field orientated coordinates. It contains two current controllers (d and q) shown in Fig. 7. The phase currents $i_{u,v,w}$ are transformed into the field orientated current values i_d and i_q. Using a modified look-up table (New LUT) the set values for the current controllers are calculated. In contrast to the common MTPA/MTPV strategy the set values are not only dependent on the desired torque t_{set} and the actual speed n but also on a set value of the current amplitude $\hat{i}_{set}$ calculated by the temperature control system. The derivation of its calculation will be explained in the following sections. Additionally,

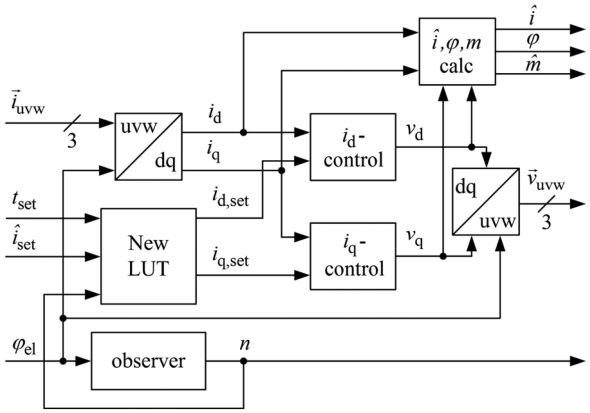

FIGURE 7. Torque control system.

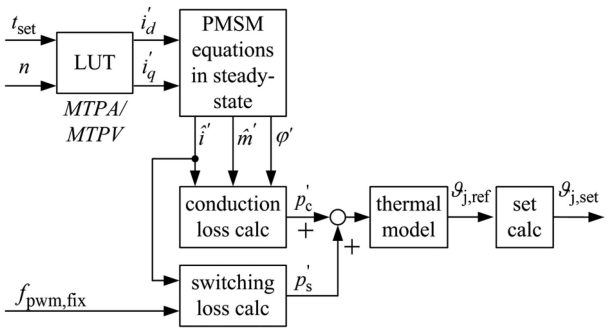

FIGURE 8. Set value calculation of the junction temperature $\vartheta_{j,set}$.

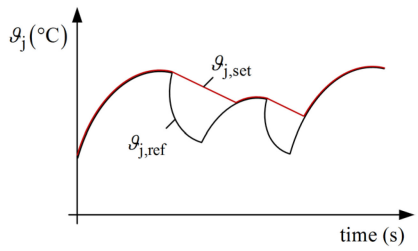

FIGURE 9. Principle of the set value calculation.

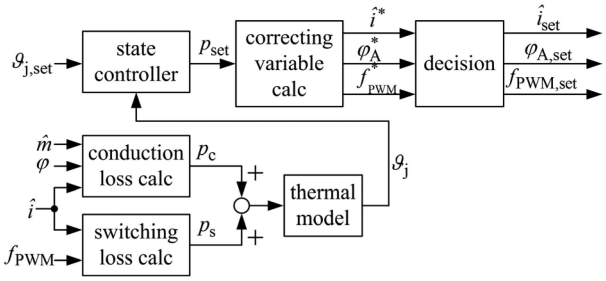

FIGURE 10. Junction temperature controller.

the actual values of the current amplitude $\hat{i}$, the amplitude of the modulation range $\hat{m}$ and the phase shift φ between the fundamentals of the output phase currents and voltages are necessary to estimate the actual power losses p and as a result the junction temperature ϑ_j.

The set value of the junction temperature $\vartheta_{j,set}$ is determined by calculating a reference junction temperature $\vartheta_{j,ref}$ under the assumption of reference operation conditions. These reference conditions relate to either the MTPA or the MTPV strategy, the modulation strategy DPWM and a fixed switching frequency $f_{pwm,fix}$ of 15 kHz. The switching and conduction power losses p'_s and p'_c under these reference operation conditions are calculated. They are the input variables for the thermal model [29] which estimates the junction temperature resulting in the reference junction temperature $\vartheta_{j,ref}$, see Fig. 8. The value of the current amplitude $\hat{i}'$, the amplitude of the modulation range $\hat{m}'$and the phase shift φ' are derived with the help of the equations of the IPMSM in steady state. If the reference temperature $\vartheta_{j,ref}$ course and the set value temperature $\vartheta_{j,set}$ course have previously been rising then the new set value of the junction temperature $\vartheta_{j,set}$ is to be equal with the actual reference temperature $\vartheta_{j,ref}$ value. If the reference temperature $\vartheta_{j,ref}$ course starts to fall then the set value $\vartheta_{j,set}$ is defined to fall with a predefined slope until it matches the reference temperature $\vartheta_{j,ref}$ again, see Fig. 9. The gradient's value affects how much the temperature control system influences the increase of the expected lifetime. A flatter slope leads to a bigger increase of the lifetime, but also to less efficiency because more additional losses are generated during low load conditions. The value of the gradient must not be zero. Otherwise the set value would never decrease, which leads to a very high set value after some time. This is not suitable for lifetime extension and it is very inefficient.

The main component of the temperature control system is a second order state controller. The junction temperature ϑ_j is calculated on the basis of the actual switching frequency f_{PWM}, the phase shift φ, the amplitude of the current $\hat{i}$ and the modulation range $\hat{m}$. The power losses p_s and p_c are fed to a second thermal model in order to estimate the actual junction temperature ϑ_j [29]. The temperature controller calculates the control variable first in the form of power losses p_{set}, see Fig. 10. The power losses p_{set} are then converted to the related control variables $\hat{i}^*$, φ^*_A and f^*_{PWM}. This is achieved by rearranging the power loss equations to these variables. The equations further require the actual values of f_{PWM}, φ, $\hat{i}$ and $\hat{m}$, but for simplicity they are not shown in the block diagram. Finally, in order to select the actuating variables, it has to be decided which control variable is active to be changed by the temperature controller. The decision procedure is depicted in Fig. 11.

If the clamping area φ_A is the active control variable, the switching frequency f_{PWM} is set to 15 kHz and the current amplitude $\hat{i}$ is set according to the MMPA/MTPV strategy. The estimated length of the clamping area φ^*_A is used.

If the clamping area φ_A is suggested to be smaller than zero, which is not possible, then the current amplitude $\hat{i}$ as actuating variable takes over. In this case the switching frequency f_{PWM}

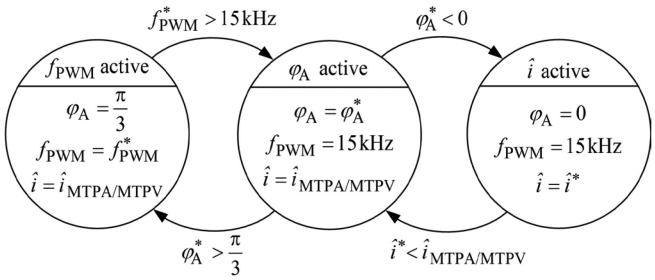

FIGURE 11. Decision procedure of the temperature controller for selection of the active control variables.

is again set to 15 kHz and the length of the clamping area φ_A is set to zero. The estimated current amplitude $\hat{i}^*$ is used. If the estimated current amplitude $\hat{i}^*$ is smaller than the amplitude calculated with the MTPA/MTPV strategy then the clamping area φ_A takes over as the control variable again.

If the estimated clamping area φ^*_A is larger than $\frac{\pi}{3}$, the switching frequency f_{PWM} is the new control variable. In this case the current amplitude $\hat{i}$ is set again to the MTPA/MTPV strategy and the length of the clamping area φ_A is set fixed to $\frac{\pi}{3}$. The estimated switching frequency f^*_{PWM} is used. If it is larger than 15 kHz then the length of the clamping area φ_A takes over again. In short, the clamping area φ_A and the current amplitude are used as control variables to reduce the temperature swings by increasing the power losses. The switching frequency f_{PWM} is only used to prohibit an overshoot in the junction temperature ϑ_j during the transitions between low and high load conditions.

In order to achieve a control system which guarantees maximum efficiency of the whole drive system the selection of the default control set values is of utmost importance. This predefinition relies on consideration of all loss effects – including losses of the motor drive and the power electronic system. Side effects such as e.g., EMI must not be neglected.

The control behaviour siginificantly relies on the precision of the model parameters. For being able to compensate control deviation the control systems include integral parts. However, also some share of negative control reserve is necesarry to compensate for such deviation. Therefore, at least one of the afore introduced actuating variables needs to include negative control reserve. Within this work the switching frequency f_{PWM} is chosen. The default value of 15 kHz is configured in accordance with EMI, loss, and current ripple considerations. It is not the lowest possible configuration but includes negative control reserve. As a matter of course also the default values of φ_A or $\hat{i}$ can be configured to include negative control reserve. The need for this is application specific.

IV. EXPERIMENTAL SETUP AND RESULTS

A. TEST SETUP

The test setup used for validation of the temperature control-principles and system consists of a 30 kW asynchronous machine (ASM) mechanically coupled to a 70 kW interior permanent magnet synchronous machine (IPMSM). The data is depicted in the Tables 1 and 2. The ASM is speed controlled and the IPMSM is torque controlled.

The ASM and the IPMSM are each driven with two-level three-phase inverters. All are water cooled. The test inverter of the IPMSM is equipped with opened (none encapsulated) and blackened (for easier temperature measurement) IGBT-power-modules, see Fig. 12 and Table 3. for the device type

TABLE 2. Parameters ASM

Symbol	Quantity	Value
R_S	stator resistance	12.6 mΩ
R_r	rotor resistance (prim.)	6.9 mΩ
L_M	main field inductance	0.119 mH
L_S	leakage inductance	0.052 mH
z_p	pole pairs	2
t_{rated}	rated torque	38 Nm
p_{rated}	rated power	30 kW
n_{rated}	rated speed	7500 rpm

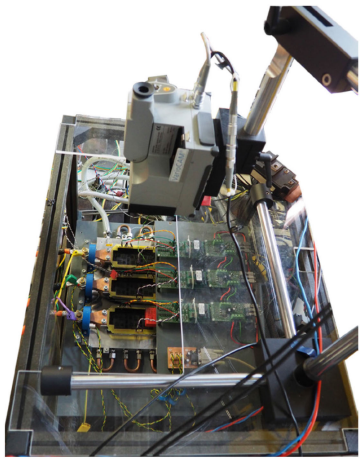

FIGURE 12. Two-level three-phase inverter with opened and blackened IGBT-power modules and IR-camera.

TABLE 3. Parameters IGBT-module: Infineon FF300R12ME4

Symbol	Quantity		Value
$I_{C,norm}$	rated collector current		300 A
V_{CES}	reverse collector-emitter voltage		1200 V
Foster network parameters IGBT (junction to case)			
r_1	0.00582 K/W	T_1	0.01 s
r_2	0.03201 K/W	T_2	0.02 s
r_3	0.03104 K/W	T_3	0.05 s
r_4	0.02813 K/W	T_4	0.1 s

as well as the electrical and thermal parameters of the IGBT-power-module. With an IR-camera it is possible to monitor the mean area-related chip-temperature of the power semiconductors. The used IR-camera is the model VarioCAM from InfraTec. It has a spectral range of (7.5..14) μm, a temperature measuring range of (−40..1200)°C and a temperature resolution at 30°C of below 0.08 K. Its precision is given by the datasheet with ±2% with a possible offset error of ±2 K. It uses a sampling frequency of 50 Hz. The offset is calibrated by an offset correction to match the specific operating measurement range.

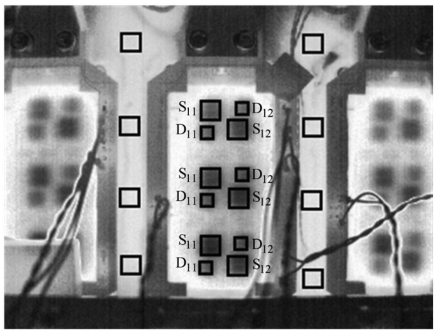

FIGURE 13. Area related mean temperature of the semiconductor devices.

B. EXPERIMENTAL RESULTS

1) EXPLANATION TO THE EVALUATION OF THE MEASUREMENTS

The principle functionality of the junction temperature control system is demonstrated at a constant speed of 1000 rpm and at alternating torque patterns between 10 Nm and 50 Nm.

The three individual control variables, namely the switching frequency f_{PWM}, the length of the clamping area φ_{A} and the current amplitude $\hat{\imath}$ are influenced by the model-based control system.

Case 1 represents the length of the clamping area φ_{A} as control variable, case 2 represents the variable switching frequency f_{PWM} and case 3 represents the presetting of the current amplitude $\hat{\imath}$. Finally, the results of the combined application of all three control variables will be addressed (case 4: combination).

The investigations are designed to establish the impact of reducing the temperature swings and the loss energy consumption of the inverter and of the machine. In all of the following figures the dotted lines represent the reference curves where no temperature control system is active. The black solid lines represent the curves with an active temperature control system applied. The grey solid lines show the temperature set value of the IGBT S_{11}. At this point it should be remembered that the conditions of the reference measurements are the application of the DPWM method with a fixed length of the clamping area $\varphi_{\mathrm{A}} = \frac{\pi}{3}$, the desired torque is set according to the MTPA/MTPV strategy and the switching frequency is fixed at $f_{\mathrm{PWM}} =$ 15 kHz. The temperature courses depicted in the following figures show the mean area temperature of the semiconductor devices S_{11} and D_{11}, each containing three chips, see Fig. 13.

As mentioned earlier the IR-camera is only used to evaluate the chip surface temperature and has no influence on the system behavior. Its sampling frequency does not allow temperature fluctuations in the range of the switching frequency beyond ∼10 Hz to be visualized. However, the influence of micro temperature swings for this work is neglectable as it demonstrates the methodology, compare [30].

The evaluation of the temperature curves with regard to the expected lifetime is carried out by using the rainflow algorithm [31] which considers the magnitude of temperature swings $\Delta\vartheta_{\mathrm{j}}$ and their mean temperatures $\vartheta_{\mathrm{j,m}}$ to calculate their number of appearances. The expected cycles to failure N_{f} of each temperature swing is estimated by using the LESIT-lifetime model [2], see Eqn. 1. The caused damage Q_x of a certain occurring temperature swing $\Delta\vartheta_{\mathrm{j,x}}$ is calculated by the ratio of the number this magnitude temperature swing $N_{\mathrm{s},x}$ and its corresponding number of cycles to failure $N_{\mathrm{f,x}}$. The caused damage of all thermal cycles $1 \ldots n$ within the temperature curves Q_{SUM} is calculated with the Palgrem-Miner rule for a linear damage accumulation, see Eqn. (2).

$$Q_{\mathrm{SUM}} = \sum_{\mathrm{x}=1}^{n} Q_{\mathrm{x}} = \sum_{\mathrm{x}=1}^{n} \frac{N_{\mathrm{x}}}{N_{\mathrm{f,x}}} \tag{2}$$

The IGBT S_{11} is the semiconductor device which temperature is controlled, but it is possible to choose any one of the other semiconductor devices. The IGBTs have a higher overall damage Q_{SUM} than the diodes at this specific load pattern. Therefore, it is reasonable to control any one of the IGBT's junction temperature because in this case they determine the expected lifetime of the entire IGBT-power-module. The overall damages strongly depend on the load pattern; nevertheless, this simple load pattern gives a good impression on the potential of the different control variables.

2) CASE 1: φ_{A} AS A CONTROL VARIABLE

The temperature control system uses only the length of the clamping area φ_{A} as actuating variable to increase the power losses at low load conditions. The torque is alternating with the described pattern, the current amplitude $\hat{\imath}$ is alternating in the same manner as the MTPA/MTPV-strategy is applied and the switching frequency is fixed at 15 kHz, see Fig. 14. The temperature curves of all the semiconductor devices show a reduction of the magnitude of the temperate swings $\Delta\vartheta_{\mathrm{j}}$ and an increase of their mean temperatures $\vartheta_{\mathrm{j,m}}$. The overall damage Q_{SUM} of these measurements can be seen in Fig. 18. The overall damage Q_{SUM} has been reduced by the temperature control system. The overall damage Q_{SUM} of the IGBTs is reduced by about 56% and that of the diodes by about 52%. The temperature control system using this control variable is not capable to follow the set value of the junction temperature $\vartheta_{\mathrm{j,set}}$. It reaches its limits during the low load conditions

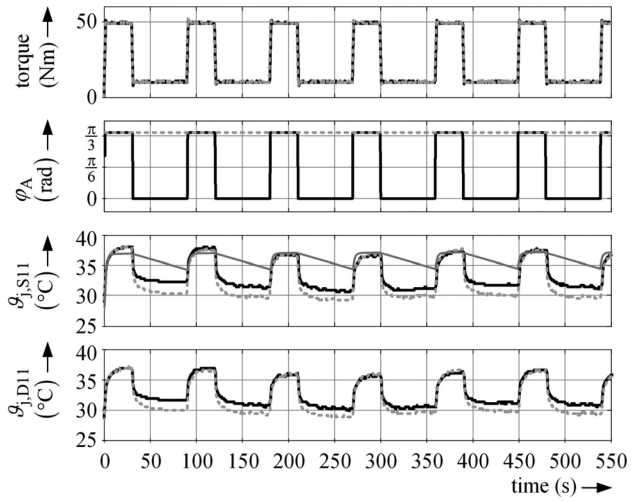

FIGURE 14. Measurement results from the temperature control system using only the length of the clamping area φ_A as control variable.

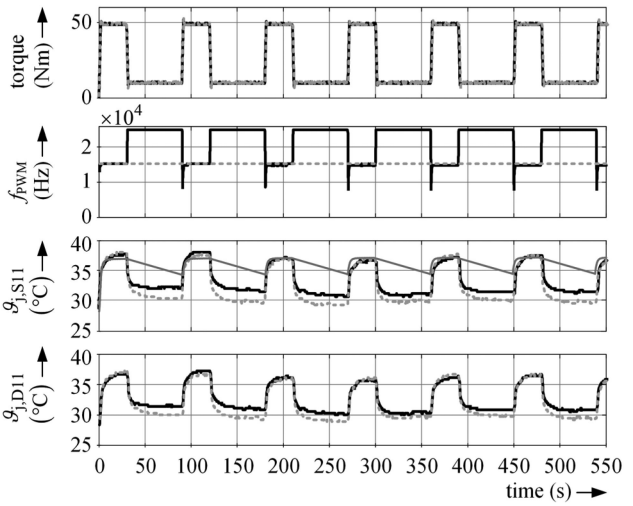

FIGURE 15. Measurement results from the temperature control system using only the switching frequency f_{PWM} as control variable.

since the additional power losses strongly depend on the current amplitude in the low load conditions. The energy losses in the inverter are increased by around 17%, see Fig. 19. The energy losses in the IPMSM are reduced by about 2%. The maximum possible power losses are generated at a zero length of the clamping area $\varphi_A = 0$, in that case the modulation waves are equal to those of the SVPWM strategy. The current ripple of the SVPWM strategy is lower when compared to the DPWM strategies [27]. This explains the reduction of energy losses in the IPMSM. The mean efficiency of the whole drive system with an inactive temperature control system is by 80.2%. The overall mean efficiency with active temperature control system drops to 78.5%.

3) CASE 2: f_{PWM} AS A CONTROL VARIABLE

The upper limit of the switching frequency is set to $f_{PWM} = 25$ kHz. This choice is defined by limits of cooling, EMI and precision of the selected microcontroller which realizes control and modulation. Therefore, it is application specific and at this point should be considered exemplary. As the switching losses strongly depend on the current amplitude $\hat{i}$ at the actual load condition, the control system is forced to its limit, see Fig. 15. It yields a smaller reduction of the overall damage Q_{SUM} of the semiconductor devices compared to the previous shown control variable, but it is around the same magnitude. For the IGBTs the damage reduction is approximately 52% and for the diodes it is about 46%, see Fig. 18. The loss energy of the inverter has increased by 19%. The loss energy in the IPMSM has been slightly reduced, as a higher switching frequency f_{PWM} results in a lower current ripple. The control variables presented have the benefit that the losses of the IPMSM do not increase. The mean efficiency of the overall drive system in this case is 78.5% and is about 2% lower than it would be without the junction temperature controller.

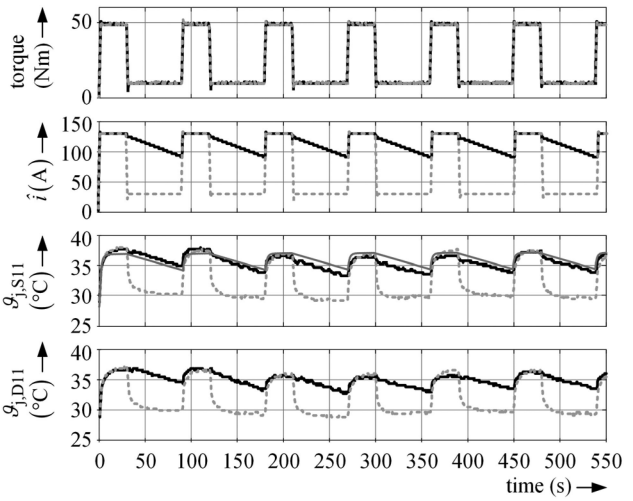

FIGURE 16. Measurement results from the temperature control system using only the current amplitude $\hat{i}$ as control variable.

4) CASE 3: CURRENT AMPLITUDE $\hat{i}$ AS A CONTROL VARIABLE

This control variable, unlike the two previous control variables, does not reach the limits of its range. In Fig. 16 one can observe that the junction temperatures of all semiconductor devices follow the predefined slope of the set value calculation.

The small deviation between the temperature set value and the real-time temperature measured with the IR-camera comes from calculation errors of the power loss and thermal models. This leads to a wrong real-time temperature value, which is fed back to the controller. The main reason for these errors is the change of the heat sink and ambient temperature, which are not considered in the thermal model. The deviation between the set value and the junction temperature measured with the IR-camera is below 2 K. However, the deviation

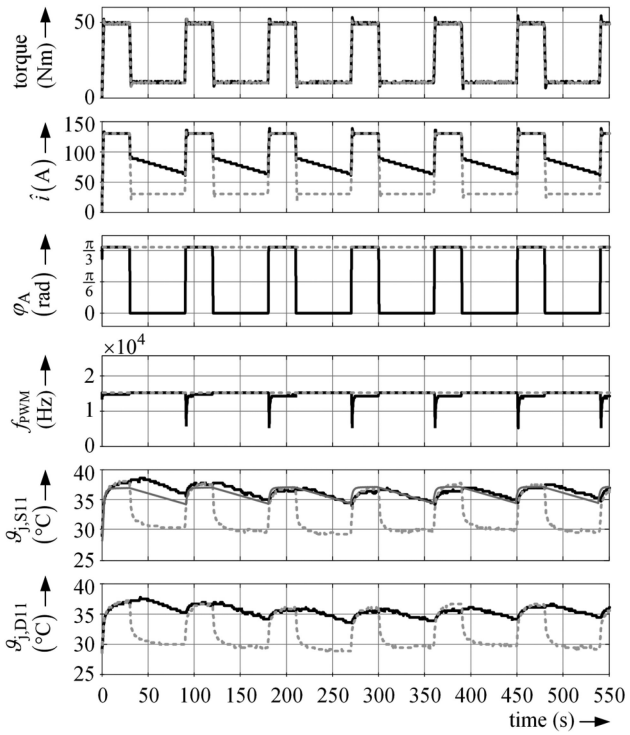

FIGURE 17. Measurement results from the temperature control system using all three control variables (φ_A, f_{PWM} and $\hat{i}$).

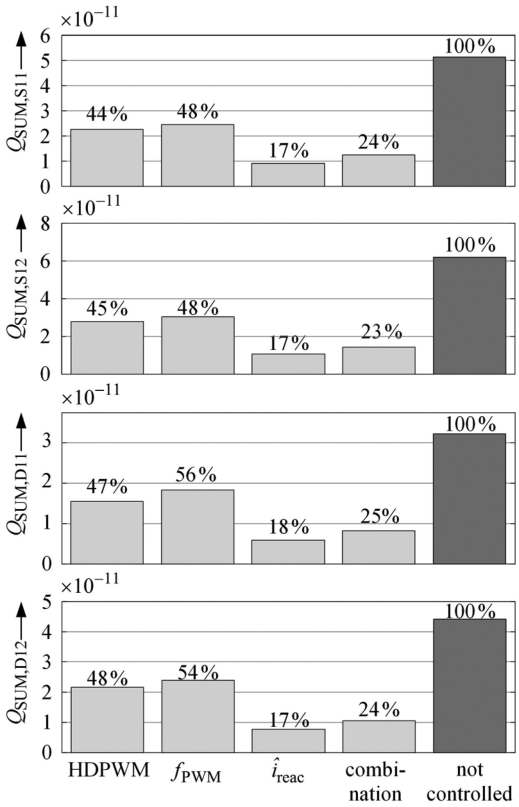

FIGURE 18. Overall damages Q_{SUM} of all semiconductors.

could be reduced by tracking the heat sink temperature and considering it in the thermal model.

The overall damage Q_{SUM} is reduced by 83% for the IGBTs and the diodes within the test cycle, see Fig. 18. The energy losses of the inverter are higher than in the two previous cases. However, energy losses in the IPMSM are significantly increased, by 32% as depicted in Fig. 19. In the IPMSM the ohmic losses, eddy currents and hysteresis losses depend on the current amplitude. While the magnitude of the temperature swings $\Delta\vartheta_j$ is reduced in the desired manner, the higher power losses in the IPMSM are a clear drawback. The overall drive system mean efficiency is 7% lower as without a temperature control system.

5) CASE 4: COMBINATION OF ALL THREE CONTROL VARIABLES

In Fig. 17 the results of a combination of all three control variables are depicted. The junction temperature courses follow the predefined slope of the set value calculation. Again, there is a small deviation between set value and measured temperature by IR-camera. The reasons are inaccuracies in the real-time temperature calculation as mentioned before. The afore mentioned negative control reserve becomes necessary when all control variables are combined. The switching frequency f_{PWM} is reduced when the junction temperature starts to rise in order to prohibit an overshoot of the junction temperature ϑ_j. The additional power losses in low load condition are realized first by reducing the length of the clamping area φ_A which quickly reaches its limit, and then the imprint of a specific current amplitude takes over. It is visible that a lower current value is required. Unexpectedly, the inverter energy losses are higher than in case 3. As the courses of the set values of the junction temperatures are identical, the power losses should be the same. A more detailed analysis of the measured area-related mean junction temperature courses of the semiconductor devices reveals a slight overshoot between the transition of the high load and the low load condition, leading to more power losses than required. The reason is inaccuracy of the analytic power loss equations, as the inverter produces more power losses than calculated in the transient condition. Nevertheless, the overall damage Q_{SUM} is reduced by about 77% for the IGBTs and the diodes. The reduction is lower as in case 3 due to the previous mentioned overshoot of the area-related mean junction temperatures. Fig. 19 illustrates that the loss energy in the IPMSM has been reduced by about 19 percentage points compared to case 3. The overall drive train mean efficiency is at 73.22%, which is 7% lower without a temperature control system active. Due to the undesired additional losses in the inverter the mean efficiency is similar as in case 3. The potential in reducing the energy losses in the IPMSM by combining the actuating variables is demonstrated.

V. SUMMARY AND CONCLUSION

This paper presents a junction temperature control system with the aim to reduce the temperature swings of the semiconductor devices in IGBT-power-modules, caused through

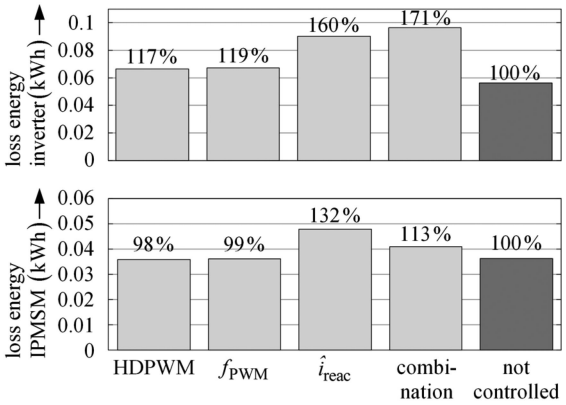

FIGURE 19. Energy losses in the inverter and the IPMSM.

load changes by increasing the power losses during low load conditions and lifting the lower junction temperature at the semiconductor devices. The increase in power losses in the IGBT-power-modules are influenced by controlling three different operating variables of the inverter. Application of a HDPWM strategy to vary the length of the clamping area φ_A, the variation of the switching frequency f_{PWM} and the preset of a specific current amplitude $\hat{i}$ by creating a reactive current component. The functionality of the proposed temperature control system to reduce temperature swings has been verified by measurements on a 30 kW motor test setup with a three-phase 300 A/1200 V inverter. The functionality of this control strategy has been demonstrated on basic load change cycles and measurements for three different control variables and their combination have been shown. In this paper the measurement results are shown for one specific slope of the junction temperature to drop during the low load conditions. However, it is possible to preset different values of the slope during low load conditions. This is equivalent to the intensity if the impact of the junction temperature control system regarding the reduction of the junction temperature swings. Drawbacks and benefits of each control variable are explained.

All presented junction temperature control systems do successfully reduce the damage to the semiconductors devices within an IGBT-power-module representing a half-bridge of the three-phase inverter and therefore increase their lifetime.

While the proposed junction control system has to create higher energy losses in the IGBT-power-modules of up to 70% compared to normal conditions, which reduces the overall mean efficiency by 7%, the estimated lifetime by the LESIT lifetime model is four times longer.

Future work on this topic could focus on implementing the presented principles to other power electronics circuit applications and topologies or to improve the lifetime of the semiconductor devices by the application of optimal control strategies.

REFERENCES

[1] J. Lutz, H. Schlangenotto, U. Scheuermann, and R. De Donker, "Destructive mechanisms in power devices," in *Semiconductor Power Devices Physics, Characteristics, Reliability*, Heidelberg Dordrecht London: Springer NY, 2011, pp. 419–473.

[2] M. Held, P. Jacob, G. Nicoletti, P. Scacco, and M.-H. Poech, "Fast power cycling test of IGBT modules in traction application," in *Proc. Power Electron. Drive Syst.,* 1997.

[3] M. Ciappa, "Selected failure mechanisms of modern power modules," ELSEVIER Microelectronics Reliability. [Online]. 2002, Jan, vol. 42, pp. 653–667. [Online]. Available: www.sciencedirect.com/science/article/pii/S0026271402000422

[4] D. A. Murdock, J. E. R. Torres, J. J. Connors, and R. D. Lorenz, "Active thermal control of power electronic modules," *IEEE Trans. Ind. Appl.*, vol. 42, no. 2, pp. 552–558, Mar./Apr. 2006.

[5] J. Lemmens, P. Vanassche, and J. Driesen, "Optimal control of traction motor drives under electrothermal constraints," *IEEE J. Emerg. Sel. Topics Power Electron.*, vol. 2, no. 2, pp. 249–263, Jan. 2014.

[6] Y. Song and B. Wang, "Evaluation methodology and control strategies for improving reliability of HEV power electronic system," *IEEE Trans. Veh. Technol.*, vol. 63, no. 8, pp. 3661–3676, Oct. 2014.

[7] X. Wang, A. Castellazzi, and P. Zanchetta, "Regulated cooling for reduced thermal cycling of power devices," in *Proc. Int. Power Electron. Motion Control Conf. (IPEMC),* 2012.

[8] X. Wang, A. Castellazzi, and P. Zanchetta, "Temperature control for reduced thermal cycling of power devices," in *Proc. Eur. Conf. Power Electron. Appl. (EPE),* 2013.

[9] M. Weckert and J. Roth-Stielow,"Lifetime as a control variable in power electronic systems," in *Proc. Emobility – Electrical Power Train,* 2010.

[10] M. Weckert and J. Roth-Stielow, "Chances and limits of a thermal control for a three-phase voltage source inverter in traction applications using permanent magnet synchronous or induction machines," in *Proc. Eur. Conf. Power Electron. Appl. (EPE),* 2011.

[11] J. Falck, M. Andresen, and M. Liserre,"Active thermal control of IGBT power electronic converters," in *Proc. Conf. IEEE Ind. Electron. Soc. (IECON),* 2015.

[12] J. Wölfle, J. Roth-Stielow, O. Koller, and B. Bertsche, "Control method to increase the reliability of IGBT power modules validated on a three phase inverter," in *Proc. Vehicle Power Propulsion Conf. (VPPC),* 2015.

[13] J. Wölfle, O. Lehmann, and J. Roth-Stielow, "A novel control method to improve the reliability of traction inverters for permanent synchronous machines," in *Proc. Int. Conf. Power Electron. Drive Syst. (PEDS),* 2015.

[14] J. Wölfle, M. Nitzsche, J. Weimer, M. Stempfle, and J. Roth-Stielow "Temperature control system using a hybrid discontinuous modulation technique to improve the lifetime of IGBT power modules," in *Proc. Eur. Conf. Power Electron. Appl. (EPE),* 2016.

[15] Y. Yerasimou, V. Pickert, B. Ji, and X. Song, "Liquid metal magneto-hydrodynamic pump for junction temperature control of power modules," *IEEE Trans. Power Electron.*, vol. 33, no. 12, pp. 10583–10593, Dec. 2018.

[16] P. Kumar Prasobhu, V. Raveendran, G. Buticchi, and M. Liserre, "Active thermal control of GaN-based DC/DC converter," *IEEE Trans. Ind. Appl.*, vol. 54, no. 4, pp. 3529–3540, Jul.-Aug. 2018.

[17] J. Ruthardt, M. Fischer, J. Felix Woelfle, N. Troester, and J. Roth-Stielow, "Three-level-gate-driver to run power transistors in the saturation region for junction temperature control," in *Proc. PCIM Europe; Int. Exhib. Conf. Power Electron., Intell. Motion, Renewable Energy Energy Management*, Nuremberg, Germany, 2018.

[18] J. Ruthardt *et al.*, "Closed loop junction temperature control of power transistors for lifetime extension," in *Proc. IEEE Appl. Power Electron. Conf. Expo. (APEC)*, New Orleans, LA, USA, 2020, pp. 2955–2955.

[19] C. H. van der Broeck, L. A. Ruppert, R. D. Lorenz, and R. W. De Doncker, "Methodology for active thermal cycle reduction of power electronic modules," *IEEE Trans. Power Electron.*, vol. 34, no. 8, pp. 8213–8229, Aug. 2019.

[20] B. Wang, L. Zhou, Y. Zhang, K. Wang, X. Du, and P. Sun, "Active junction temperature control of IGBT based on adjusting the turn-off trajectory," *IEEE Trans. Power Electron.*, vol. 33, no. 7, pp. 5811–5823, Jul. 2018.

[21] M. Andresen, K. Ma, G. Buticchi, J. Falck, F. Blaabjerg, and M. Liserre, "Junction temperature control for more reliable power electronics," *IEEE Trans. Power Electron.*, vol. 33, no. 1, pp. 765–776, Jan. 2018.

[22] K. Ma, M. Liserre, and F. Blaabjerg, "Reactive power influence on the thermal cycling of multi-MW wind power inverter," *IEEE Trans. Ind. Appl.*, vol. 49, no. 2, pp. 922–930, Mar.-Apr. 2013.

[23] J. Wölfle and J. Roth-Stielow, "A hybrid discontinuous modulation technique to influence the switching losses of three phase inverters," in *Proc. Euro. Conf. Power Electron. Appl. (EPE),* 2015.

[24] Y. Ko, M. Andresen, G. Buticchi, and M. Liserre, "Discontinuous-modulation-based active thermal control of power electronic modules in wind farms," *IEEE Trans. Power Electron.*, vol. 34, no. 1, pp. 301–310, Jan. 2019.
[25] J. Ruthardt, J. Woelfle, M. Zehelein, and J. Roth-Stielow, "A new modulation technique to control the switching losses for single phase three-level active-neutral-point-clamped-inverters," in *Proc. PCIM Eur.; Int. Exhib. Conf. Power Electron., Intell. Motion, Renewable Energy Energy Manage.*, Nuremberg, Germany, 2017.
[26] E. Ugur, S. Dusmez, and B. Akin, "An investigation on diagnosis-based power switch lifetime extension strategies for three-phase inverters," *IEEE Trans. Ind. Appl.*, vol. 55, no. 2, pp. 2064–2075, Mar.-Apr. 2019.
[27] D. G. Holmes and A. Lipo, "Discontinuous modulation," in *Pulse Width Modulation For Power Converters Principles and Practice*, Piscataway: IEEE Press, 2003, pp. 299–336.
[28] M. Weckert and J. Roth-Stielow, "Lifetime orientated control of a three-phase voltage source inverter," in *Proc. Internal Exhib. Conf. Power Electron., Intell. Motion, Renewable Energy Energy Manage. (PCIM)*, 2010.
[29] J. Wölfle, M. Nitzsche, N. Tröster, J. Ruthardt, M. Stempfle, and J. Roth-Stielow, "Combination of two variables in a junction temperature control system to elongate the expected lifetime of IGBT-power-modules," in *Proc. IEEE 12th Int. Conf. Power Electron. Drive Syst. (PEDS)*, 2017, pp. 41–47.
[30] G. Zeng, R. Alvarez, C. Künzel, and J. Lutz, "Power cycling results of high power IGBT modules close to 50 Hz heating process," in *Proc. 21st Eur. Conf. Power Electron. Appl. (EPE '19 ECCE Europe)*, Genova, Italy, 2019.
[31] M. Matsuishi and T. Endo, "Fatigue of metals subjected to varying stress," in *Proc. Japan Soc. Mech. Eng.*, 1968.

JULIAN WÖLFLE was born in Ravensburg, Germany in 1986. He received the Diplom-Ingenieur degree in electronics from the University of Stuttgart, Germany, in 2012. He worked as a Research Associate at the Institute for Power Electronics and Electrical Drives (ILEA) of the University of Stuttgart from 2012 to 2018, with the research topic on the investigation of control methods in order to increase the reliability of power electronic semiconductor devices. Since 2018 is currently an Application Engineer at dSPACE GmbH. Mr. Wölfle is Author and Co-Author of more than 15 peer-reviewed conference papers.

MAXIMILIAN NITZSCHE (Student Member, IEEE) was born in Stuttgart, Germany in 1989. He received the B.Sc. degree and M.Sc. degree in electrical engineering from the University of Stuttgart, Germany, in 2012 and 2016, respectively. He is a Research Associate at the Institute for Power Electronics and Electrical Drives (ILEA) of the University of Stuttgart and is currently working towards the Dr.-Ing. degree. The focus of his current research is on the application of wide bandgap semiconductor devices – especially SiC – in the field of power electronics and methods to investigate their reliability. Mr. Nitzsche serves as a Reviewer for the IEEE JOURNAL OF EMERGING AND SELECTED TOPICS IN POWER ELECTRONICS and is Author and Co-Author of more than 15 peer-reviewed journal and conference papers. He is student member of the PELS.

JOHANNES RUTHARDT was born in Tübingen, Germany in 1990. He received the B.Sc. and the M.Sc. degree in electrical engineering from the University of Stuttgart, Germany, in 2013 and 2016, respectively. He currently works as a Research Associate at the Institute for Power Electronics and Electrical Drives (ILEA) of the University of Stuttgart towards the Dr.-Ing. degree. The main research topic is in the field of reliability of power semiconductor devices including real-time junction temperature measurement and junction temperature control for lifetime extension. Mr. Ruthardt is Author and Co-Author of more than 20 peer-reviewed journal and conference papers in the field of power electronics.

JÖRG ROTH-STIELOW (Member, IEEE) was born in Oberndorf a.N., Germany, in 1959. He has graduated in electrical engineering in 1984 and received the doctoral degree in 1991, both from the University of Stuttgart. In the period from 1991 to 2003, he worked as Chief Development Manager at SEW-EURODRIVE GmbH, Bruchsal, Germany, where he focused on inverter systems, electrical drives, control technology and automation systems. In 2003, he joined the University of Stuttgart as Full Professor for power electronics and electrical drives as well as Managing Director of the Institute for Power Electronics and Electrical Drives. His research interests include power electronics, control technology and electrical drives.